Effect of Metal-Support Interface on Hydrogen Permeation through Palladium Membranes

Ke Zhang
Dept. of Chemical Engineering, Arizona State University, Tempe, AZ 85287, and Tianjin Key Laboratory of Applied Catalysis Science and Technology and State Key Laboratory on Chemical Engineering (Tianjin University), School of Chemical Engineering, Tianjin University, Tianjin 300072, China

Xiaotong Wei
Dept. of Chemical Engineering, Arizona State University, Tempe, AZ 85287

Zebao Rui
Dept. of Chemical Engineering, Arizona State University, Tempe, AZ 85287, and Tianjin Key Laboratory of Applied Catalysis Science and Technology and State Key Laboratory on Chemical Engineering (Tianjin University), School of Chemical Engineering, Tianjin University, Tianjin 300072, China

Yongdan Li
Tianjin Key Laboratory of Applied Catalysis Science and Technology and State Key Laboratory on Chemical Engineering (Tianjin University), School of Chemical Engineering, Tianjin University, Tianjin 300072, China

Y. S. Lin
Dept. of Chemical Engineering, Arizona State University, Tempe, AZ 85287

DOI 10.1002/aic.11760
Published online January 16, 2009 in Wiley InterScience (www.interscience.wiley.com).

Thin palladium membranes of different thicknesses were prepared on sol-gel derived mesoporous γ-alumina/α-alumina and yttria-stabilized zirconia/α-alumina supports by a method combining sputter deposition and electroless plating. The effect of metal-support interface on hydrogen transport permeation properties was investigated by comparing hydrogen permeation data for these membranes measured under different conditions. Hydrogen permeation fluxes for the Pd/γ-Al_2O_3/α-Al_2O_3 membranes are significantly smaller than those for the Pd/YSZ/α-Al_2O_3 membranes under similar conditions. As the palladium membrane thickness increases, the difference in permeation fluxes between these two groups of membranes decreases and the pressure exponent for permeation flux approaches 0.5 from 1. Analysis of the permeation data with a permeation model shows that both groups of membranes have similar hydrogen permeability for bulk diffusion, but the Pd/γ-Al_2O_3/α-Al_2O_3 membranes exhibit a much lower surface reaction rate constant with higher activation energy, due possibly to the formation of Pd-Al alloy, than the Pd/YSZ/α-Al_2O_3 membranes. © 2008 American Institute of Chemical Engineers *AIChE J,* 55: 630–639, 2009
Keywords: Pd membrane, hydrogen permeation, metal-support interface, Pd-Al interaction

Correspondence concerning this article should be addressed to Y.S. Lin at jerry.lin@asu.edu.

Introduction

Hydrogen is a valuable industrial material, and is consumed on the order of billions of cubic meters per year as a feedstock or intermediate in a wide range of chemical, petrochemical and metallurgical processes, including hydrogenations, iron ore reduction, synthesis gas generation and production of ammonia.[1,2] There is an increased global willingness to embrace the proposed "hydrogen economy" as a potential long-term solution to the growing energy challenges as the demand for clean and efficient energy rises.[3] The purpose of this hypothetical economy is to eliminate the use of carbon-based fossil fuels, and, thus, reduce carbon dioxide emissions, to provide an energy carrier to replace dwindling supplies of petroleum, and to provide energy independence to countries without oil resources. To move toward the goal, one of the crucial issues is the availability of inexpensive, reliable and pure hydrogen.

Hydrogen is most economically produced by steam methane reforming (SMR), followed by several separation steps, such as high- and low-temperature shift conversion and pressure swing adsorption.[4] The produced hydrogen usually includes small quantities of carbon monoxide, carbon dioxide, and hydrogen sulfide as impurities that require further purification. Separations account for a large fraction of energy expenditure and capital investment in this process. Membrane separation using hydrogen selective membranes has been considered as a feasible substitute to obtaining pure hydrogen with less disbursal. Pd-based membranes have therefore attracted considerable interest on account of their perfect permeability and permselectivity for hydrogen.[5–7] Pd-based membranes also put forward the possibility of hydrogen separation at high-temperature, and application of membrane reactors aiming at combining a separation process with a chemical reaction in one unit, which are very attractive since many petrochemical processes can be enhanced by the membranes under their operation conditions.[8,9]

The earlier palladium membranes were self-supported disks or tubes (typically thicker than 200 microns) prepared by conventional metallurgical processes. Such thick metallic membranes were limited by low H_2 permeance and uneconomical usage of the precious metal. These problems can be overcome by preparing thinner membranes on top of porous glass,[10,11] ceramic[12,13] and metal substrates.[14,15] The porous substrate should in principle provide the mechanical strength for the thin metallic membrane, while imposing less transport resistance for H_2 permeation during operation. A variety of techniques are available to deposit these metallic films, including electroless plating,[16–19] magnetron sputtering,[20,21] chemical vapor deposition (CVD),[21–23] and electrodeposition.[24]

Pd and Pd-alloy membranes with thickness ranging from submicron to about 10 micrometers can be prepared by these methods described previously. However, there is no clear correlation between membrane thickness and hydrogen permeance for these Pd membranes prepared by different methods.[7] For instance, Lin and coworkers[30,31] reported H_2 permeance for the submicron-thick Pd-based membranes on γ-alumina support prepared by sputter deposition[30,31] and CVD[21–23] in the order of magnitude of 10^{-7}-10^{-8} mol/m^2. s. Pa at 573K, even lower than those for micron-thick Pd membranes on α-alumina support prepared by the electroless plated membranes ($\sim 10^{-6}$-10^{-7} mol/m^2 s Pa).[32] The activation energy for hydrogen permeation through the ultrathin Pd membranes prepared by sputter deposition, and CVD is about 30 kJ/mol, significant higher than those of reported electroless plated membranes (<20 kJ/mol).[9,13,33–38] It was suggested that such differences in the membranes were caused by the different microstructure of the membranes formed by the different preparation methods.[31] However, the aforementoned suggestion cannot explain the fact that the hydrogen permeation through the submicron-thick Pd membrane is rate-limited by the surface reaction step at a much smaller rate than for the micron-thick Pd membranes prepared by the electroless plating method.

To prepare good quality submicron-thick Pd membranes requires the use of a porous support with a smooth surface. Therefore, in the work of Lin and workers,[20–23] the large pore α-alumina supports were coated with a micron-thick mesoporous γ-alumina layer with pore size in the range of only 3–5 nm. It is possible that Pd-γ-alumina interface has a much lower hydrogen permeation surface reaction rate as compared to other Pd-support interface. To examine the effects of the metal-support interface on hydrogen transport properties requires the coating of thin Pd membranes on mesoporous supports of different materials. In this work, thin Pd membranes of identical properties were synthesized on mesoporous γ-alumina/α-alumina and yttria-stabilized-zirconia (YSZ/α-alumina support), with a pore size of about 4 nm by electroless plating method. The main objective of this work is to study the effects of metal-support interface (Pd-γ-alumina and Pd-YSZ) on hydrogen permeation mechanism through the Pd membranes.

Experimental

The porous α-alumina supports (2 mm thick with 0.2 μm average pore diameter) were prepared by pressing α-alumina powder (Alcoa, A-16), followed by a calcination process and polishing of one side.[20] An intermediate layer of γ-alumina or YSZ was coated on one side of the support disk by the sol-gel method. Boehmite sol was prepared by the procedure reported by Yoldas,[39] and YSZ sol was made according to the method of Gao et al.[18] for preparation of zirconia sol, with the procedure modified to add 0.07M yttrium nitrate (Aldrich, 99.9%) solution, to obtain 8 mol % YSZ. Both sols were mixed with 5 wt % poly (vinyl alcohol) (PVA, Fluka, MW = 72,000) to prevent crack formation during heat treatment process. The γ-alumina or YSZ layer was coated by the dip-coating on the polished surface of the support with the boehmite or YSZ sol, followed by drying at 313K and 40–50% humidity, and calcination under controlled temperature conditions.[40] The resulting γ-alumina and YSZ layer were about 2-3 μm thick, controlled by the coating time and sol concentration, with an average pore diameter of 4 nm and 3.3 nm, respectively.

Pd top layer was prepared by the electroless plating technique. The composite support was first activated to seed the surface layer with nuclei of palladium that can initiate the autocatalytic process at the start of the electroless plating. DC magnetron sputtering was used to deposit the Pd seed layer since it could ensure the uniformity and purity of the seed layer, compared to other activation methods. A palladium foil (Alfa Aesar, 99.9%) was used as the target. The

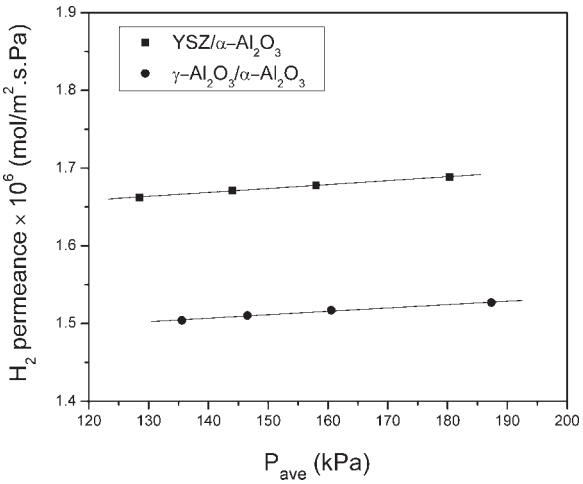

Figure 1. Average pressure dependency of H_2 permeance for γ-Al_2O_3/α-Al_2O_3 and YSZ/α-Al_2O_3 support at room-temperature.

distance between the target and surface of composite support was kept at 10 cm. Prior to the deposition, the chamber was evacuated to a pressure in the range of 10^{-6} Torr, and then back filled with ultra high purity argon at a pressure of 5×10^{-3} Torr. Palladium was sputtered at the power of 10 W for 5 min at room-temperature. The deposition rate was about 7 nm/min. After this activation process, the composite support was placed in a beaker containing Pd plating solution. The Pd plating bath consisted of $PdCl_2$ (Aldrich, 99.9+%) 20 mg/mL; Na_2EDTA (Sigma, 99%) 0.5mol/L; NH_4OH (EMD Chemicals, 28%) 350 mL/L; N_2H_4 (Aldrich), 0.206mol/L, and was kept at 333K. Thickness of 2.5 μm, 5 μm and 7.5 μm Pd membranes were obtained on both γ-Al_2O_3/α-Al_2O_3 and YSZ/α-Al_2O_3 composite supports by changing the plating time.

The gas-tightness of the electroless plated Pd membranes was confirmed by zero measurable nitrogen permeation flux at the pressure difference up to 202 KPa at room-temperature, which gives a nitrogen permeance smaller than 10^{-10} mol/m^2 s Pa, based on the permeation equipment limit. Hydrogen and nitrogen permeation experiments were carried out in a home-made steady-state permeation setup consisting of a H_2 gas cylinder, a N_2 gas cylinder, a precision pressure gauge, a needle valve, a permeation cell with the effective area of 2.0 cm^2, and a temperature programmable furnace. The schematic illustration of equipment and membrane cell used in this study has been shown in a previous article.[41] A high-temperature membrane cell with graphite seals was used to measure the permeation properties at high-temperatures. Hydrogen or nitrogen (for detecting leakage) single gas was introduced to the upstream side of the membrane, and the pressure in the upstream side was modified by the needle valve, and measured by an accurate pressure gauge. Pd composite membranes were heated to a desired temperature at a ramp rate of 0.5°C/min under inert gas atmosphere prior to H_2 permeation testing. Stable permeation fluxes were recorded. During the elevated temperature permeation experiments, nitrogen was introduced at each temperature to check the integrity of Pd membrane and sealing quality. No detectable N_2 permeation flux was measured, indicating good membrane integrity and gas tightness of the seal. The downstream flow rate was measured with a soap-bubble flow meter, and the downstream pressure was ambient atmosphere (101 kPa) without purging gas in all experiments. X-Ray diffraction (XRD, Siemens D5000 diffractometer) was used to identify the metallic crystalline structure with Cu Kα radiation. The cross-section of Pd composite membranes was characterized to determine film thickness using scanning electron microscopy (SEM, Philips X30).

Results and Discussion

Figure 1 shows H_2 permeances at various transmembrane average pressure at room-temperature for the two supports. As shown, the permeance vs. transmembrane average pressure can be correlated by a straight line

$$F = \alpha_s + \beta_s \cdot P_{av} \quad (1)$$

The slope and intercept in the figure represent the contribution of viscous flow and Knudsen diffusion, respectively.[42] The regressed values for the constant of α_s (mol/s m^2 Pa), and β_s (mol/s m^2 Pa^2) at room-temperature are, respectively, 1.60×10^{-6} and 5.06×10^{-13} for YSZ/α-Al_2O_3 and 1.45×10^{-6} and 4.37×10^{-13} for γ-Al_2O_3/α-Al_2O_3 at room-temperature. Due to similar pore structure, pressure dependence of the permeance for the two supports (values of β_s) are same. H_2 permeance of YSZ/α-Al_2O_3 (value of α_s) is only about 10% higher than that of γ-Al_2O_3/α-Al_2O_3 support, which indicates the resistance of these two supports are comparable.

Pd membranes were prepared by electroless plating technique on the γ-Al_2O_3/α-Al_2O_3 and YSZ/α-Al_2O_3 supports. Figure 2 gives the XRD patterns of 2.5 μm Pd composite membranes. It shows the presence of pure palladium in a standard fcc structure with a set of four reflections from crystalline planes 111, 200, 220 and 311 in the 30–85° 2θ range. There is no diffraction peaks from α-Al_2O_3 and YSZ layer due to coating of the Pd layer in sufficient thickness. The average Pd crystalline size calculated by Scherrer equation is 105 nm, and manifests little change when membrane thickness increases. SEM photographs showing the cross-section of Pd/γ-Al_2O_3/α-Al_2O_3 and Pd/YSZ/α-Al_2O_3 membrane are

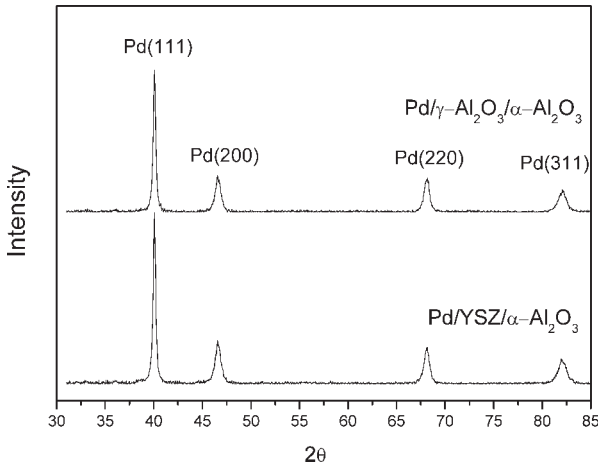

Figure 2. XRD patterns of the 2.5 μm Pd composite membranes.

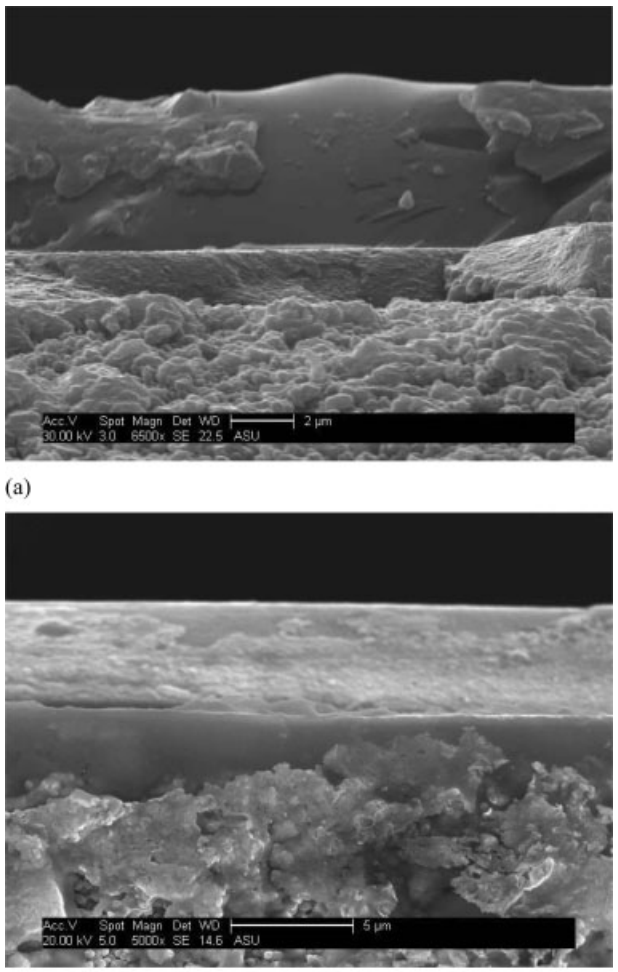

Figure 3. Cross-section SEM photographs of (a) 5 μm Pd/γ-Al_2O_3/α-Al_2O_3, and (b) 5 μm Pd/YSZ/α-Al_2O_3.

illustrated in Figure 3. It clearly shows the composite structure with Pd top layer, γ-Al_2O_3/YSZ intermediate layer and base α-Al_2O_3 support.

Figure 4a and b show H_2 flux of 2.5 μm Pd membranes on the two supports with a different intermediate layer as a function of pressure difference in a temperature range of 633–713K. Note that P_h is the upstream hydrogen pressure of Pd side, and P_l is the downstream hydrogen pressure of the support side. As shown, H_2 flux through Pd/YSZ/α-Al_2O_3 membrane is two to three times higher than that through Pd/γ-Al_2O_3/α-Al_2O_3 membrane. It can be seen that the H_2 flux increases with increasing temperature and is proportional to the feed and permeate side pressure difference.

Comparing to the results in Figure 4 with those in Figure 1, the hydrogen permeance through Pd-support composite membranes is 45–55% of support permeance for Pd/YSZ/α-Al_2O_3, and 15-25% for Pd/γ-Al_2O_3/α-Al_2O_3 membrane, respectively. This indicates that support contributes significantly to the resistance of hydrogen permeation. To obtain hydrogen permeance through Pd layer only, hydrogen pressure at metal-support interface, P_m, is calculated by the resistance in series model as:

$$P_m = \left[\left(\frac{\alpha_s}{\beta_s}\right)^2 + 2P_l \cdot \left(\frac{\alpha_s}{\beta_s}\right) + P_l^2 + \frac{2J}{\beta_s}\right]^{1/2} - \frac{\alpha_s}{\beta_s} \quad (2)$$

where J is hydrogen permeation flux. The permeation coefficients α_s and β_s were obtained by regressing Eq. 1 with the permeance data for the supports at the corresponding temperatures. The resulting H_2 permeation flux through Pd layer vs. transmembrane pressure difference across Pd layer only (P_h-P_m), is illustrated in Figure 5 for the membranes shown in Figure 4. From the results, one can easily obtain permeance for Pd layer only from $Q/(P_h$-$P_m)$.

H_2 permeation flux through a metal membrane at a given temperature is usually described by the following equation[7]

$$J = k\left(P_h^n - P_m^n\right) \quad (3)$$

where k is permeation coefficient, L the metal membrane thickness, and n the H_2 pressure exponent. The value of n indicates the rate-limiting step of H_2 permeation through Pd membranes. If the bulk diffusion of atomic hydrogen is rate-determining step, n equals to 0.5. When surface process involving the H_2 dissociative adsorption on Pd membrane and/or atomic H recombination and desorption at the perme-

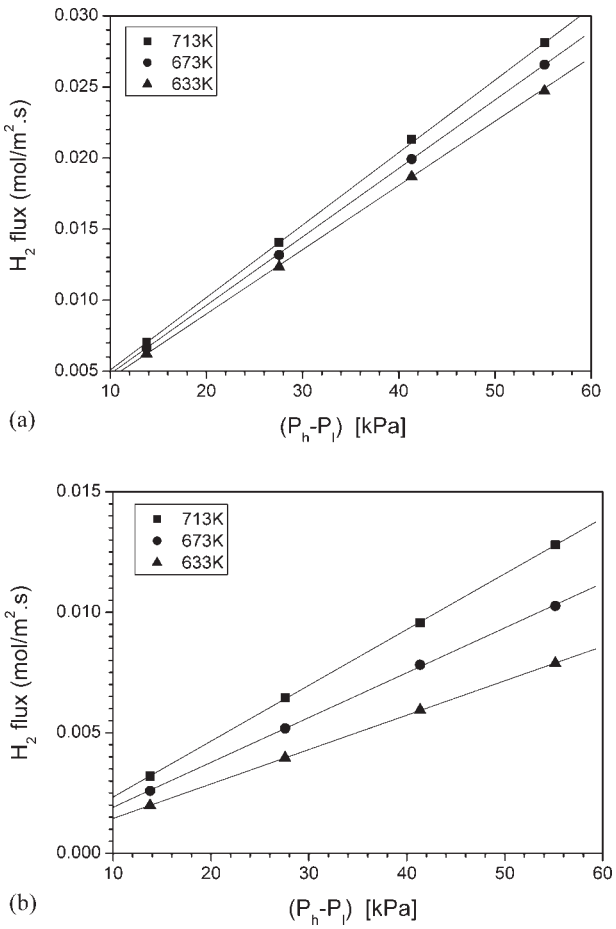

Figure 4. H_2 permeation flux of 2.5 μm Pd composite membranes as a function of pressure difference at various temperatures: (a) Pd/YSZ/α-Al_2O_3 and (b) Pd/γ-Al_2O_3/α-Al_2O_3.

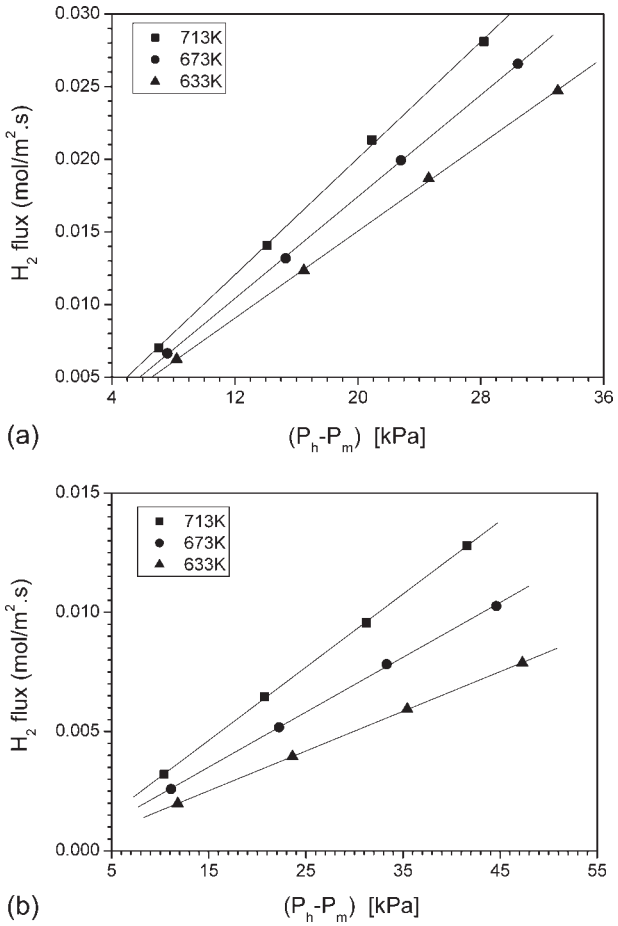

Figure 5. (a) H_2 permeation flux of 2.5 μm Pd layer (Pd/YSZ/α-Al_2O_3) as a function of P_h-P_m, and (b) H_2 permeation flux of 2.5 μm Pd layer (Pd/γ-Al_2O_3/α-Al_2O_3) as a function of P_h-P_m.

ate side controls the H_2 permeation, n is 1. When both the surface process and bulk diffusion are responsible for determining H_2 permeation rate, n will vary between 0.5 and 1.

The results given in Figure 5 show an n value of 1 for the 2.5 μm thick Pd membranes on both the supports. This indicates that surface reaction is the rate-limiting step. Similar results for the 5 μm and 7.5 μm thick Pd membranes are given in Figures 6 and 7, respectively. The value of n decreases from 1 to above 0.6, with increasing Pd membrane thickness. This indicates that for the thinnest Pd membranes, the surface reaction rate is rate-limiting, and the importance of bulk-diffusion resistance increases with increasing Pd membrane thickness. Pd membranes on the surface of YSZ not only have a higher permeance, but also relatively less resistance offered by the surface reaction step as indicated by a smaller value of n for Pd membrane of the same thickness as compared to Pd membranes on γ-alumina support.

The ratio of H_2 flux through Pd/YSZ/α-Al_2O_3 to that through Pd/γ-Al_2O_3/α-Al_2O_3 composite membrane is shown in Figure 8 as a function of Pd layer thickness. The H_2 flux values are compared instead of H_2 permeances in this figure at the same upstream and downstream pressure, and the same temperature because the pressure exponent n for different thickness membranes is not the same. It is difficult to compare permeances with different unit of pressure difference (driving force) in one figure. As shown in Figure 8, the difference in H_2 flux between the two membranes decreases as the membrane thickness increases. It is known that metal-support interaction takes place at the interface of Pd layer and ceramic support. Such interaction can affect H_2 permeation rate when the bulk diffusion step is not rate-limiting. As membrane thickness increases, the rate-limiting step gradually transforms from surface process to bulk diffusion as indicated by the change of pressure exponent n. When bulk diffusion of atomic hydrogen plays a more important role, what happens on the Pd surface would be less significant due to the shift in permeation resistance to the bulk Pd. When membrane thickness increases from 2.5 μm to 7.5 μm, the pressure exponent n for Pd/YSZ/α-Al_2O_3 decreases to a greater extent from 1 to 0.65 than that for Pd/γ-Al_2O_3/α-Al_2O_3 from 1 to 0.78.

In order to identify the true difference in Pd membranes through the Pd membranes on these two supports, the permeation data should be analyzed by a more accurate permeation model. According to the model derived by Lin and

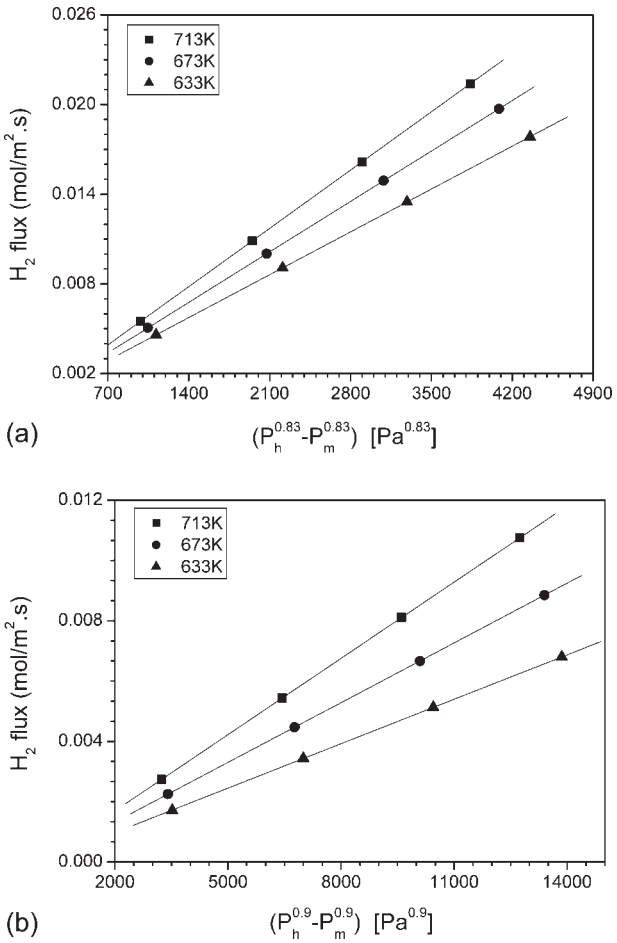

Figure 6. (a) H_2 permeation flux of 5 μm Pd layer (Pd/YSZ/α-Al_2O_3) as a function of pressure difference at various temperatures, and (b) H_2 permeation flux of 5 μm Pd layer (Pd/γ-Al_2O_3/α-Al_2O_3) as a function of pressure difference at various temperatures.

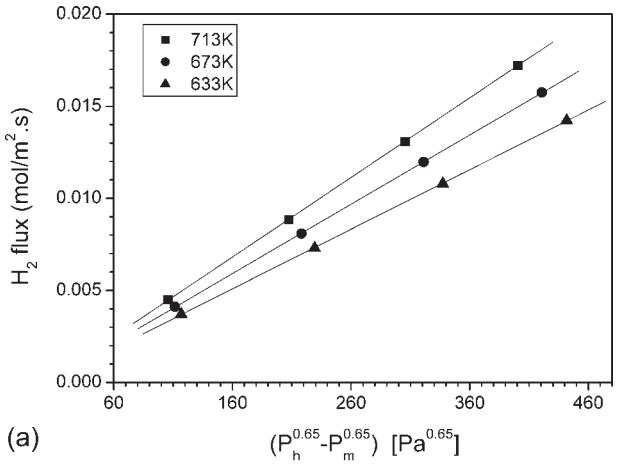

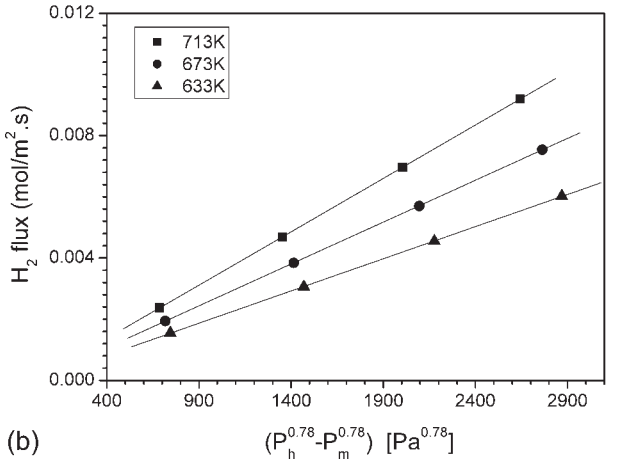

Figure 7. (a) H_2 permeation flux of 7.5 μm Pd layer (Pd/YSZ/α-Al_2O_3) as a function of pressure difference at various temperatures, and (b) H_2 permeation flux of 7.5 μm Pd layer (Pd/γ-Al_2O_3/α-Al_2O_3), as a function of pressure difference at various temperatures.

coworkers,[43,44] H_2 permeation through a thin Pd membrane can be described by the following equations.

At the upstream gas-membrane interface

$$J = \alpha_1 (P_h - P_{h'}) \tag{4}$$

In bulk palladium

$$J = \alpha_2 \left(P_{h'}^{0.5} - P_{m'}^{0.5}\right) \tag{5}$$

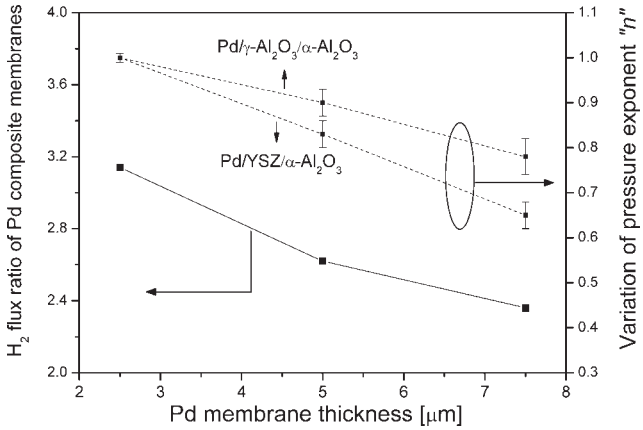

Figure 8. Membrane thickness dependency of H_2 flux ratio through Pd/YSZ/α-Al_2O_3 to that through Pd/γ-Al_2O_3/α-Al_2O_3 (Temperature: 633 K; P_h: 156.5 KPa; P_l: 101.3 KPa), and pressure exponent variation.

At the membrane-support interface

$$J = \alpha_3 (P_{m'} - P_m) \tag{6}$$

where α represents rate constants in each step; $P_{h'}$ and $P_{m'}$ are H_2 partial pressure on Pd membrane surfaces. Note that

$$\alpha_2 = \frac{f}{L} \tag{7}$$

where f is the permeability of the bulk Pd membrane.

H_2 dissociative adsorption on the Pd surface proceeds much faster than the other two steps.[45–47] Therefore, Eq. 4 can be neglected and $P_{h'}$ is the same as P_h. Solving Eqs. 5 and 6 gives

$$P_{m'} = \left(\frac{-\alpha_2 + \sqrt{\alpha_2^2 + 4\alpha_3^2 P_m + 4\alpha_2 \alpha_3 P_h^{0.5}}}{2\alpha_3} \right)^2 \tag{8}$$

and

$$J = \alpha_3 \left[\left(\frac{-\frac{f}{L} + \sqrt{\left(\frac{f}{L}\right)^2 + 4\alpha_3^2 P_m + 4\left(\frac{f}{L}\right)\alpha_3 P_h^{0.5}}}{2\alpha_3} \right)^2 - P_m \right] \tag{9}$$

Thus, Eq. 9 correlates H_2 flux J to P_h, P_m, L, f, and rate constant α_3. At a given temperature, the value of f and α_3 can be obtained by regressing Eq. 9 with H_2 flux data for

Table 1. Regressed f and α_3 of Hydrogen Permeation through Pd Membranes

	Pd/YSZ/α-Al_2O_3		Pd/γ-Al_2O_3/α-Al_2O_3	
T (K)	f (mol/m s $Pa^{0.5}$)	α_3 (mol/m^2 s Pa)	f (mol/m s $Pa^{0.5}$)	α_3 (mol/m^2 s Pa)
713	$(3.01\pm0.22)\times10^{-9}$	$(2.61\pm0.19)\times10^{-6}$	$(2.25\pm0.36)\times10^{-9}$	$(4.15\pm0.07)\times10^{-7}$
673	$(2.58\pm0.20)\times10^{-9}$	$(2.35\pm0.18)\times10^{-6}$	$(1.93\pm0.49)\times10^{-9}$	$(3.02\pm0.07)\times10^{-7}$
633	$(2.17\pm0.19)\times10^{-9}$	$(2.14\pm0.17)\times10^{-6}$	$(1.72\pm0.39)\times10^{-9}$	$(2.05\pm0.03)\times10^{-7}$

membranes of the three different thicknesses. The regression was performed by Matlab R2006b (MathWorks, Inc., Natick, U.S.), with a trust region method, which is based on interior-reflective Newton method,[48,49] and the results are listed in Table 1. The uncertainties were obtained from the least-squared regression for the parameters with 95% confidence intervals. The regressed f and α_3 values have error ranges of $\pm$1–9% except for f of Pd/γ-Al_2O_3/α-Al_2O_3 membranes, with error ranges of $\pm$16–25%. The larger error in f is due to errors associated with Pd membrane thicknesses. The experimental measured H_2 flux for Pd membranes are compared in a parity plot in Figure 9, to calculated H_2 flux by applying P_h, P_m, L, and regressed f and α_3 to Eq. 9. It is shown that the model is an excellent match to the experimental data with a correlation coefficient of 0.9996.

The data in Table 1 shows that the permeability value for bulk diffusion for both membranes are similar considering the experimental errors. The values for the surface reaction rate constant α_3 Pd/γ-Al_2O_3/α-Al_2O_3 membrane are about one-order of magnitude smaller than those for Pd/YSZ/α-Al_2O_3 membranes. Figure 10 illustrates Arrhenius plots of f and α_3 for the membranes on the two supports. Both f and α_3 increase with increasing temperatures, reflecting the activated nature of the permeation process. Regression by Arrhenius equation for f and α_3 data shown in Figure 10, give the calculated activation energy for bulk Pd (designated as E_b), and for membrane-support surface reaction (designated as E_s). As shown in Table 2, E_b is similar for these two kinds of Pd membranes, while E_s for Pd/γ-Al_2O_3/α-Al_2O_3 is much higher than that of Pd/YSZ/α-Al_2O_3. From these results, it is clear that the difference in hydrogen permeance between these two membranes is caused by the surface process at the metal-support interface. For Pd/γ-Al_2O_3/α-Al_2O_3, γ-Al_2O_3 is chemically active, and may interact with Pd, resulting in the formation of a Pd-Al alloy layer which lowers surface reaction rate with increased activation energy for hydrogen transport. In comparison, such an alloy layer might not form for Pd/YSZ/α-Al_2O_3 membrane since yttria or zirconia is more inert and stable as the support than γ-alumina.

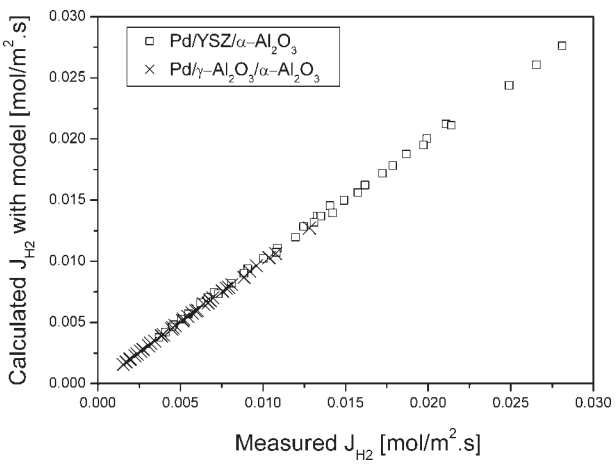

Figure 9. Comparison of measured H_2 flux with model predictions.

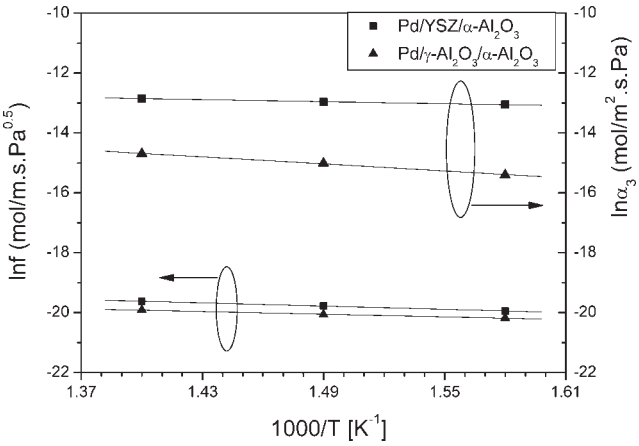

Figure 10. Arrhenius plots of f and α_3 for Pd membranes on different supports.

The investigation of Pd-Al metal-substrate interaction presented evidence during the past decade for the formation of Pd-Al alloy at a high-temperature reduction atmosphere, even though alumina is generally considered to be an inert, nonreactive support.[50] Up to now, Pd-Al alloy formation has been observed upon depositing Pd on both polycrystalline Al surfaces,[51,52] Al films,[53,54] and Al (001) single crystals, and has also been tackled by a variety of different methods, including XRD,[55] X-ray photoelectron spectroscopy,[51,52,56,57] ion scattering,[56,57] thermal desorption spectroscopy,[51,52,57] secondary ion mass spectroscopy,[51,57] CO adsorption[51,52,57,58] and transmission electron microscopy.[59] Meanwhile, Wang et al.[60] measured H_2 solubility and diffusivity for Pd-Al alloys and pure Pd at 423–503 K. It was found that Pd-Al alloys possessed lower H_2 solubility and diffusivity than that of pure Pd. Moreover, H_2 solubility and diffusivity decreases with atomic Al fraction increases. While the temperatures used in this work are higher than 503 K, it is believed the variation tendency should be the same. H_2 flux decreases as Pd-Al alloy is formed at the interface between Pd layer and support, based on the fact that H_2 permeability is the product of diffusivity and solubility. Therefore, combined with our current results, one may conclude that Pd-Al metal-support interaction is an alloy formation process that increases surface activation energy E_s, and decreases H_2 permeability for Pd membranes.

Table 3 summarizes the apparent activation energy for hydrogen permeation (obtained by regressing the hydrogen permeance at different temperatures with the Arrhenius equation) for different Pd-based membranes published in the literature. For electroless plated Pd membranes or cold rolling Pd disks, the activation energy lies between 8–15 kJ/mol if bulk diffusion is a rate-limiting step, or both bulk diffusion and

Table 2. Bulk and Surface Activation Energy Calculated by f and α_3 for Hydrogen Permeation through Different Pd Membranes

	E_b (kJ/mol)	E_s (kJ/mol)
Pd/YSZ/α-Al_2O_3	15.1	9.17
Pd/γ-Al_2O_3/α-Al_2O_3	12.4	32.6

Table 3. Comparison of Activation Energy for Hydrogen Permeation through Pd-based Membranes Reported in the Literature

Membrane	Preparation method	Thickness (μm)	Activation Energy (kJ/mol)	n-value	Reference
Pd disk	Cold rolling	27–154	11.9	0.68	[33]
Pd disk	Cold rolling	50	11.4	n/a	[34]
$Pd_{77}Ag_{23}/Al_2O_3$	Electroless plating	8.6	8.22	0.5	[35]
Pd/Al_2O_3	Electroless plating	11.4	8.88	0.58	[13]
Pd-Ag/α-Al_2O_3	Electroless plating	5.5	9.80	0.61	[36]
Pd/Al_2O_3	Electroless plating	15.0	10.0	0.65	[9]
Pd/porous glass	Electroless plating	13.0	10.7	n/a	[37]
Pd/α-Al_2O_3	Electroless plating	10.3	12.3	0.65	[38]
$Pd_{77}Ag_{23}/\gamma$-Al_2O_3	Sputtering	0.35	23.0	n/a	[20]
$Pd_{75}Ag_{25}/\gamma$-Al_2O_3	Sputtering	0.1–1.5	27.9–32.0	n/a	[21]
Pd/γ-Al_2O_3	Electroless plating	3	15.8	1	[61]

surface process are responsible for determining the whole permeation process.[9,13,33–38] The activation energy for bulk diffusion E_b obtained in this work is in good agreement with the reported values. For thin Pd membranes prepared on γ-Al_2O_3 layer with surface process being dominant, the activation energy is higher (>15 kJ/mol), with the values for sputtered thin films[20,21] being larger than the electroless plated one.[61] The main difference between thin Pd membranes prepared by sputtering and electroless plating is the membrane microstructure with different Pd grain size. The grain size for sputtering method is about 10–20 nm,[31] while it is usually larger than 100 nm for electroless plated one.[62] Note that the Pd seed layer (30–40 nm thickness) before electroless plating in this work was obtained by the sputtering technique. The smaller grain size tends to induce a more significant Pd-Al metal-support interaction for sputtered Pd membranes that increases H_2 permeation resistance further.

Conclusions

Defect-free Pd composite membranes were prepared by the combination of sputter deposition and electroless plating on porous ceramic support coated with sol-gel derived mesoporous γ-alumina or yttria stabilized zirconia (YSZ) as the intermediate layer. The effect of metal-support interface on hydrogen transport permeation properties was investigated by comparing hydrogen permeation data through palladium membranes of different thicknesses on these two supports at different temperatures and hydrogen pressures. Hydrogen permeation fluxes for the Pd/γ-Al_2O_3/α-Al_2O_3 membrane are significantly smaller than those for the Pd/YSZ/α-Al_2O_3 under similar conditions including membrane thickness. As the membrane thickness increases from 2.5 μm to 7.5 μm, the difference in the H_2 flux between the Pd membranes on the two supports decreases because the bulk diffusion plays a more important role in determining the H_2 permeation rate, as indicated by the change of pressure exponent n for Pd/YSZ/α-alumina decreasing from 1 to 0.65, and that for Pd/γ-alumina/α-alumina from 1 to 0.78. The permeation data can be analyzed by a permeation model considering both bulk diffusion and surface reaction at the metal-support interface. The results show that both membranes have similar hydrogen permeability for bulk diffusion, and that the Pd/γ-Al_2O_3/α-Al_2O_3 membrane exhibits a much lower surface reaction rate constant with higher activation energy (due possibly to the formation of Pd-Al alloy) than the Pd/YSZ/α-Al_2O_3 membrane.

Acknowledgments

This work was supported by Department of Energy (DE-FG36-07GO17001) and Petroleum Research Fund (Administered by ACS). KZ and RZ are grateful to China Scholarship Council for fellowship to support their visit to ASU. The collaboration was supported by National Natural Science Foundation of China (No.20425619), Program of Introducing Talents to University Disciplines (No. B06006) and the Program for Changjiang Scholars and Innovative Research Teams in Universities under file number IRT 0641.

Notation

E_b = activation energy for the bulk diffusion, $J \cdot mol^{-1}$
E_s = activation energy for surface process at the interface between Pd layer and support, $J \cdot mol^{-1}$
J = hydrogen flux, $mol \cdot m^{-2} \cdot s^{-1}$
k = permeability coefficient, $mol \cdot m^{-1}.s^{-1}.Pa^{-n}$
L = membrane thickness, m
P_h = hydrogen partial pressure at feed (upstream) side, Pa
P_m = hydrogen partial pressure at the interface between Pd layer and composite support, Pa
P_l = hydrogen partial pressure at permeate (downstream) side, Pa
$P_{h'}$ = hydrogen partial pressure at upstream Pd membrane surface, Pa
$P_{m'}$ = hydrogen partial pressure at downstream Pd membrane surface, Pa
f = hydrogen permeability, $mol \cdot m^{-1} \cdot s^{-1} \cdot Pa^{-n}$
R = gas constant, $J\ mol^{-1}\ K^{-1}$
T = absolute temperature, K
α_1 = rate constant for H_2 dissociative adsorption at gas-membrane interface, $mol \cdot m^{-2} \cdot s^{-1} \cdot Pa^{-1}$
α_2 = rate constant for H_2 bulk diffusion in palladium membrane, $mol \cdot m^{-2} \cdot s^{-1} \cdot Pa^{-0.5}$
α_3 = rate constant for H_2 recombinative desorption at membrane-support interface, $mol \cdot m^{-2} \cdot s^{-1} \cdot Pa^{-1}$

Literature Cited

1. Armor JN. The multiple roles for catalysis in the production of H_2. *Appl Catal A*. 1999;176:159–176.
2. Li A, Grace JR, Lim CJ. Preparation of thin Pd-based composite membrane on planar metallic substrate. Part I. The pre-treatment of the porous stainless steel substrate. *J Membr Sci*. 2007;298:175–181.
3. Ockwig NW, Nenoff TM. Membranes for hydrogen separation. *Chem Rev*. 2007;107:4078–4110.
4. Li A, Grace JR, Lim CJ. Preparation of thin Pd-based composite membrane on planar metallic substrate. Part II. Preparation of membranes by electroless plating and characterization. *J Membr Sci*. 2007;306:159–165.
5. Uemiya S. State-of-the-art of supported metal membranes for gas separation. *Sep Purif Methods*. 1999;28:51–85.
6. Lin YS. Microporous and dense inorganic membranes: current status and prospective. *Sep Purif Technol*. 2001;25:39–55.
7. Paglieri SN, Way JD. Innovation in palladium membrane research. *Sep Purif Methods*. 2002;31:1–169.

8. Shu J, Grandjean BPA, Van Neste A, Kaliaguine S. Catalytic palladium-based membrane reactors: a review. *Can J Chem Eng*. 1991;69:1036–1060.
9. Dittmeyer R, Höllein V, Daub K. Membrane reactors for hydrogenation and dehydrogenation processes based on supported palladium. *J Mol Catal A: Chem*. 2001;173:135–184.
10. Uemiya S, Sato N, Ando H, Kude Y, Matsuda T, Kikuchi E. Separation of hydrogen through palladium thin film supported on a porous glass tube. *J Membr Sci*. 1991;56:303–313.
11. Souleimanova RS, Mukasyan AS, Varma A. Effects of osmosis on microstructure of Pd-composite membranes synthesized by electroless plating technique. *J Membr Sci*. 2000;166:249–257.
12. Uemiya S, Matsuda T, Kikuchi E. Hydrogen permeable palladium-silver alloy membrane supported on porous ceramics. *J Membr Sci*. 1991;56:315–325.
13. Collins JP, Way JD. Preparation and characterization of a composite palladium-ceramic membrane. *Ind Eng Chem Res*. 1993;32:3006–3013.
14. Govind R, Atnoor D. Development of a composite palladium membrane for selective hydrogen separation at high temperature. *Ind Eng Chem Res*. 1991;30:591–594.
15. Jemaa N, Shu J, Kaliaguine S, Grandjean BPA. Thin palladium film formation on shot peening modified porous stainless steel substrate. *Ind Eng Chem Res*. 1996;35:973–977.
16. Zhao HB, Pflanz K, Gu JH, Li AW, Stroh N, Brunner H, Xiong GX. Preparation of palladium composite membranes by modified electroless plating procedure. *J Membr Sci*. 1998;142:147–157.
17. Li A, Liang W, Hughes R. Fabrication of defect free Pd/α-Al_2O_3 composite membranes for hydrogen separation. *Thin Solid Films*. 1999;350:106–112.
18. Gao HY, Lin YS, Li YD, Zhang BQ. Electroless plating synthesis, characterization and permeation properties of Pd-Cu membranes supported on ZrO_2 modified porous stainless steel. *J Membr Sci*. 2005;265:142–152.
19. Zhang K, Gao HY, Rui ZB, Li YD, Lin YS. Preparation of thin palladium composite membranes and application to hydrogen/nitrogen separation. *Chin J Chem Eng*. 2007;15:643–647.
20. Jayaraman V, Lin YS, Pakala M, Lin RY. Fabrication of ultrathin metallic membranes on ceramic supports by sputter deposition. *J Membr Sci*. 1995;99:89–100.
21. Xomeritakis G, Lin YS. Fabrication of thin metallic membranes by MOCVD and sputtering. *J Membr Sci*. 1997;133:217–230.
22. Xomeritakis G, Lin YS. Fabrication of a thin palladium membrane supported in a porous ceramic substrate by chemical vapor deposition. *J Membr Sci*. 1996;120:261–272.
23. Xomeritakis G, Lin YS. CVD synthesis and gas permeation properties of thin palladium/alumina membranes. *AIChE J*. 1998;44:174–183.
24. Nam SE, Lee KH. Hydrogen separation by Pd alloy composite membranes: introduction of diffusion barrier. *J Membr Sci*. 2001;192:177–185.
25. Roa F, Way JD, McCormick RL, Paglieri SN. Preparation and characterization of Pd-Cu composite membranes for hydrogen separation. *Chem Eng J*. 2003;93:11–22.
26. Gao HY, Lin YS, Li YD, Zhang BQ. Chemical stability and its improvement of palladium-based metallic membranes. *Ind Eng Chem Res*. 2004;43:6920–6930.
27. Roa F, Way JD. The effect of air exposure on palladium-copper composite membranes. *Appl Surf Sci*. 2005;240:85–104.
28. Ayturk ME, Mardilovich IP, Engwall EE, Ma YH. Synthesis of composite Pd-porous stainless steel membranes with a Pd/Ag intermetallic diffusion barrier. *J Membr Sci*. 2006;285:385–394.
29. Wang WP, Pan XL, Zhang XL, Yang WS, Xiong GX. The effect of co-existing nitrogen on hydrogen permeation through thin Pd composite membranes. *Sep Purif Technol*. 2007;54:262–271.
30. McCool B, Xomeritakis G, Lin YS. Composition control and hydrogen permeation characteristics of sputter deposited palladium-silver membranes. *J Membr Sci*. 1999;161:67–76.
31. McCool BA, Lin YS. Nanostructured thin palladium-silver membranes: effects of grain size on gas permeation properties. *J Mater Sci*. 2001;36:3221–3227.
32. Rothenberger KS, Cugini AV, Howard BH, Killmeyer RP, Ciocco MV, Morreale BD, Enick RM, Bustamante F, Mardilovich IP, Ma YH. High pressure hydrogen permeance of porous stainless steel coated with a thin palladium film via electroless plating. *J Membr. Sci*. 2004;244:55–68.
33. Hurlbert RC, Konecny JO. Diffusion of hydrogen through Palladium. *J Chem Phys*. 1961;34:655–658.
34. Jung SH, Kusakabe K, Morooka S, Kim SD. Effects of co-existing hydrocarbons on hydrogen permeation through a palladium membrane. *J Membr Sci*. 2000;170:53–60.
35. Guo Y, Lu G, Wang Y, Wang R. Preparation and characterization of Pd-Ag/ceramic composite membrane and application to enhancement of catalytic dehydrogenation of isobutane. *Sep Purif Technol*. 2003;32:271–279.
36. Hou K, Hughes R. Preparation of thin and highly stable Pd/Ag composite membranes and simulative analysis of transfer resistance for hydrogen separation. *J Membr Sci*. 2003;214:43–55.
37. Uemiya S, Sato N, Kude Y, Matsuda T, Kikuchi K. Separation of hydrogen through palladium thin film supported on a porous glass tube. *J Membr Sci*. 1991;56:303–313.
38. Li AW, Liang WQ, Hughes R. Fabrication of dense palladium composite membranes for hydrogen separation. *Catal Today*. 2000;56:45–51.
39. Yoldas BE. Alumina sol preparation from alkoxides. *Ceram Bull*. 1975;54:289–290.
40. Chang CH, Gopalan R, Lin YS. Thermal and hydrothermal stability study of alumina, titania and zirconia ceramic membranes. *J Membrane Sci*. 1994;91:27–45.
41. Kanezashi M, O'Brien J, Lin YS. Thermal stability improvement of MFI-type zeolite membranes with doped zirconia intermediate layer. *Micropor Mesopor Mater*. 2007;103:302–308.
42. Lin YS, Burggraaf AJ. Experimental studies on pore size change of porous ceramic membranes after modification. *J Membr Sci*. 1993;79:65–82.
43. Lin YS, Wang W, Han J. Oxygen permeation through thin mixed-conducting solid oxide membranes. *AIChE J*. 1994;40:786–798.
44. Han J, Xomeritakis G, Lin YS. Oxygen permeation through thin zirconia/yttria membranes prepared by EVD. *Solid State Ionics*. 1997;93:263–272.
45. Zhao Z, Sevryugina Y, Carpenter MA, Welch D, Xia H. All-optical hydrogen-sensing materials based on tailored palladium alloy thin films. *Anal Chem*. 2004;76:6321–6326.
46. Lewis FA. *The palladium hydrogen system*. New York: Academic Press; 1967.
47. Wei X, Wei T, Xiao H, Lin YS. Nano-structured Pd-long period fiber grating integrated optical sensor for hydrogen detection. *Sensors and Actuators B*. accepted for publication.
48. Coleman TF, Li Y. An interior, trust region approach for nonlinear minimization subject to bounds. *SIAM J Optimization*. 1996;6:418–445.
49. Coleman TF, Li Y. On the convergence of reflective Newton methods for large-scale nonlinear minimization subject to bounds. *Math Program*. 1994;67:189–224.
50. Tsud N, Veltruska K, Matolin V. Pd Interaction with Reduced Thin-Film Alumina: XPS and ISS Study. *J Catal*. 2001;204:372–377.
51. Matolinova I, Johanek V, Skala T, Veltruska K, Matolin V. XPS, TDS and static SIMS studies of binary Pd/Al system properties: correlation between Pd-Al bimetallic interaction and CO adsorption. *Appl Surf Sci*. 2005;245:87–93.
52. Johanek V, Tsud N, Matolin V, Stara I. TPD and XPS study of the CO adsorption on transition-SP metal systems: Pd and Al. *Vacuum*. 2001;63:15–22.
53. Jiang LQ, Ruckman MW, Strongin M. Experimental evidence for room-temperature intermetallic compound formation at the Pd/Al interface. *Phys Rev B*. 1989;39:1564–1568.
54. Nemsak S, Masek K, Matolin V. RHEED study of the growth of Pd-Al/MgO bimetallic system. *Vacuum*. 2005;80:102–107.
55. Kepinski L, Wolcyrz M, Jablonski JM. Effect of high-temperature reduction on carburization of alumina-supported palladium: Evidence for palladium-aluminium alloy formation. *Appl Catal*. 1989;54:267–276.
56. Shutthanandan V, Saleh AA, Shivaparan NR, Smith RJ. Growth of ultrathin Pd films on Al(001) surfaces. *Surf Sci*. 1996;350:11–20.

57. Johanek V, Stara I, Matolin V. Role of Pd-Al bimetallic interaction in CO adsorption and catalytic properties of bulk PdAl alloy: XPS, ISS, TDS, and SIMS study. *Surf Sci*. 2002;507–510:92–98.
58. Frick B, Jacobi K. Growth and electronic structure of ultrathin palladium films on Al(111) and their interaction with oxygen and carbon monoxide. *Phys Rev B*. 1988;37:4408–4414.
59. Penner S, Jeneweinl B, Hayekl K. Pd-Al interaction at elevated temperatures: a TEM and SAED study. *Catal Lett*. 2007;113:65–72.
60. Wang D, Flanagan TB, Shanahan KL. Hydrogen permeation measurements of partially internally oxidized Pd-Al alloys in the presence and absence of CO. *J Membr Sci*. 2005;253:165–173.
61. Pan XL, Xiong GX, Sheng SS, Stroth N, Brunner H. A thin dense Pd membrane supported on α-Al_2O_3 hollow fiber. *Chem Commun*. 2001;24:2536–2537.
62. Yeung KL, Christiansen SC, Varma A. Palladium composite membranes by electroless plating technique: Relationships between plating kinetics, film microstructure and membrane performance. *J Membr Sci*. 1999;159:107–122.

Manuscript received May 26, 2008, revision received Aug. 30, 2008, and final revision received Oct. 26, 2008.